

Shell model level structure of ^{216}Fr

R. K. Sheline

Departments of Chemistry and Physics, Florida State University, Tallahassee, Florida 32306

C. F. Liang and P. Paris

Centre de Spectrométrie Nucléaire et de Spectrométrie de Masse, Bâtiment 104, 91405 Campus Orsay, France

A. Gizon

Institut des Sciences Nucléaire, IN2P3, Université Joseph Fourier, F-38026 Grenoble, France

(Received 24 July 1996)

Sources of ^{220}Ac in secular equilibrium with ^{221}Pa were produced using the reaction $^{209}\text{Bi}(^{18}\text{O},3n)^{224}\text{Pa}$. The alpha decay of ^{220}Ac and coincident gamma and electron spectra were used to study the level structure of ^{216}Fr . The levels in ^{216}Fr can be interpreted in terms of the $\pi(h_{9/2})^5_{9/2}\nu(g_{9/2})^3_{9/2}$, $\pi(h_{9/2})^4_0(f_{7/2})_{7/2}\nu(g_{9/2})^3_{9/2}$, and $\pi(h_{9/2})^5_{9/2}\nu(g_{9/2})^2_0(i_{11/2})_{11/2}$ shell model configurations. The alpha decay hindrance factors of the ground state to ground state transitions in the sequence $^{224}\text{Pa}\rightarrow^{220}\text{Ac}\rightarrow^{216}\text{Fr}\rightarrow^{212}\text{At}$ suggest the collapse of quadrupole-octupole Nilsson orbitals into the more degenerate shell model orbitals. The sequence of hindrance factors in this odd chain are mirrored in the corresponding odd proton and odd neutron sequences beginning with ^{223}Pa and ^{223}Th , respectively. [S0556-2813(97)06003-2]

PACS number(s): 21.60.Cs, 23.60.+e, 27.80.+w

I. INTRODUCTION

Recently, evidence for the onset of reflection asymmetry in ^{216}Fr was obtained using the reaction $^{208}\text{Pb}(^{11}\text{B}, 3n)^{216}\text{Fr}$ [1]. A band structure with interleaved positive and negative parity states connected by enhanced $B(E1)$ transitions was observed.

Since this evidence of reflection asymmetry just eight particles beyond the double closed shell in ^{208}Pb is quite intriguing, the level structure of ^{216}Fr deserves further study. We note that the heavy ion spectroscopy populates only high spin states in ^{216}Fr [1] with the lowest state populated postulated to be the 9^- state with presumably considerable $\pi(h_{9/2})^5_{9/2}\nu(g_{9/2})^3_{9/2}$ character. Furthermore, it has been assumed [2] that the alpha decay of the ^{216}Fr ground state which populates the 1^- ground state of ^{212}At with hindrance factor (HF) 2.5 must also have spin-parity 1^- . Thus the postulated 9^- state, which is not observed to alpha decay, should ultimately be connected with the ^{216}Fr ground state through a series of low-energy highly converted transitions.

It therefore would be of considerable interest to see if we can find the connection between the high spin states and the known low spin states. Even more important is to determine whether the band structure with evidence of reflection asymmetry is also observed in the low lying low spin states.

Fortunately, the nucleus ^{220}Ac alpha decays with $\sim 100\%$ probability to energetically low lying states with presumably relatively low spins including the ground state in ^{216}Fr [3]. Since gamma transitions between the states have not been observed, only the 1^- ground state spin has previously been proposed.

^{224}Pa , a 0.76s alpha emitter (redetermined in this study) is a convenient parent of ^{220}Ac ($t_{1/2}=26.1$ ms).

The alpha and coincident gamma decays of ^{220}Ac would thus appear to be an excellent way to study ^{216}Fr . However,

in view of the short half-life of ^{220}Ac (26.1 ms), an ideal way to study ^{220}Ac is in secular equilibrium with ^{224}Pa .

It should however be noted that the alpha decay of ^{220}Ac can be expected to populate only a limited range of excitation and spin in ^{216}Fr . Given this fact the combined octupole shell model structure of the alpha decaying ground state of ^{220}Ac would emphasize the shell model states in ^{216}Fr in contrast to the collective states previously studied [1].

II. EXPERIMENTAL METHODS AND RESULTS

Sources of ^{224}Pa with ^{220}Ac in secular equilibrium were produced using the reaction $^{209}\text{Bi}(^{18}\text{O},3n)$. Self-supporting 1.5 mg/cm^2 ^{209}Bi targets were bombarded with a 96 MeV ^{18}O beam and a current of $\sim 0.6\ \mu\text{A}$ using the Grenoble SARA accelerator. A He-jet system transported the activity to a tape transport which in turn positioned the activity in front of two different experimental set ups.

In one arrangement the tape moved the activity between alpha and gamma planar Ge detectors in 180° close geometry. The alpha detector had a full width at half maximum resolution of 17 keV, while the resolution of the gamma detector was ~ 600 eV at 100 keV. Singles alpha and singles gamma spectra and alpha-gamma coincidence measurements were simultaneously recorded.

In the other arrangement the ^{224}Pa activity was moved into the uniform field of a magnetic selector which deflected the electrons onto a cooled 6 mm thick Si(Li) detector, 700 mm^2 in area with a resolution of 2 keV. Two additional coax Ge gamma and alpha detectors were available for coincidence measurements. Singles alpha and electron spectra and alpha-electron, alpha-gamma, and electron-gamma coincidence measurements were recorded simultaneously. Appropriate to the 0.8s half-life of ^{224}Pa , collection measurement cycles of 2s were used.

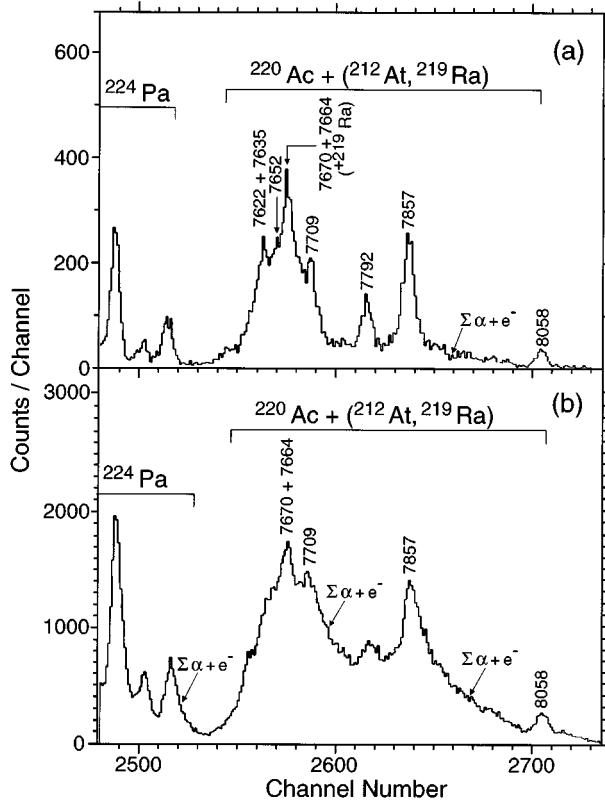


FIG. 1. The alpha spectra in coincidence with all gamma rays from a ^{224}Pa source. Alphas from ^{224}Pa and from ^{220}Ac (with ^{212}At and ^{219}Ra impurities) are bracketed. Energies of the ^{220}Ac alphas leading to states in ^{216}Fr are labeled with their energies in keV. Figure 1(a) utilizes $\Omega/4\pi = 3\%$ while Fig. 1(b) has $\Omega/4\pi = 25\%$. See text for more detail.

The alpha spectra in coincidence with all gamma rays are shown in Figs. 1(a) and 1(b). ^{224}Pa alphas are bracketed. The alphas of ^{220}Ac leading to states in ^{216}Fr , together with impurities of ^{212}At and ^{219}Ra , are also bracketed, with individual alphas of ^{220}Ac labeled with their energies in keV. Figure 1(a) shows the alpha spectrum with smaller solid angle ($\Omega/4\pi=3\%$) and therefore fewer counts but better resolution. Figure 1(b) shows the same alpha spectrum with $\Omega/4\pi = 25\%$ and poorer resolution. The larger solid angle leads to a larger alpha-electron sum continuum as indicated in Fig. 1(b) which is largely responsible for the poorer resolution.

The gamma ray spectrum in coincidence with the alpha spectrum region labeled $^{220}\text{Ac} + (^{212}\text{At}, ^{219}\text{Ra})$ in Figs. 1(a) and 1(b) is presented in Fig. 2 in four sections (a, b, c, d). Individual gamma rays of ^{216}Fr are labeled in keV and sum lines resulting from the accidental coincidences of the 133 keV gamma and Fr K x rays are labeled with an asterisk. Francium x rays, ^{208}Bi , and ^{215}Rn gamma ray impurities are also labeled.

The conversion electron spectrum in coincidence with the alpha spectrum labeled $^{220}\text{Ac} + (^{212}\text{At}, ^{219}\text{Ra})$ in Fig. 1(a) and 1(b) is shown in Fig. 3. Individual electron peaks are labeled by the energies in keV together with their K, L, M, and N assignments.

One of the most powerful methods of developing the level scheme of ^{216}Fr is shown in Figs. 4 and 5. Figure 4 repre-

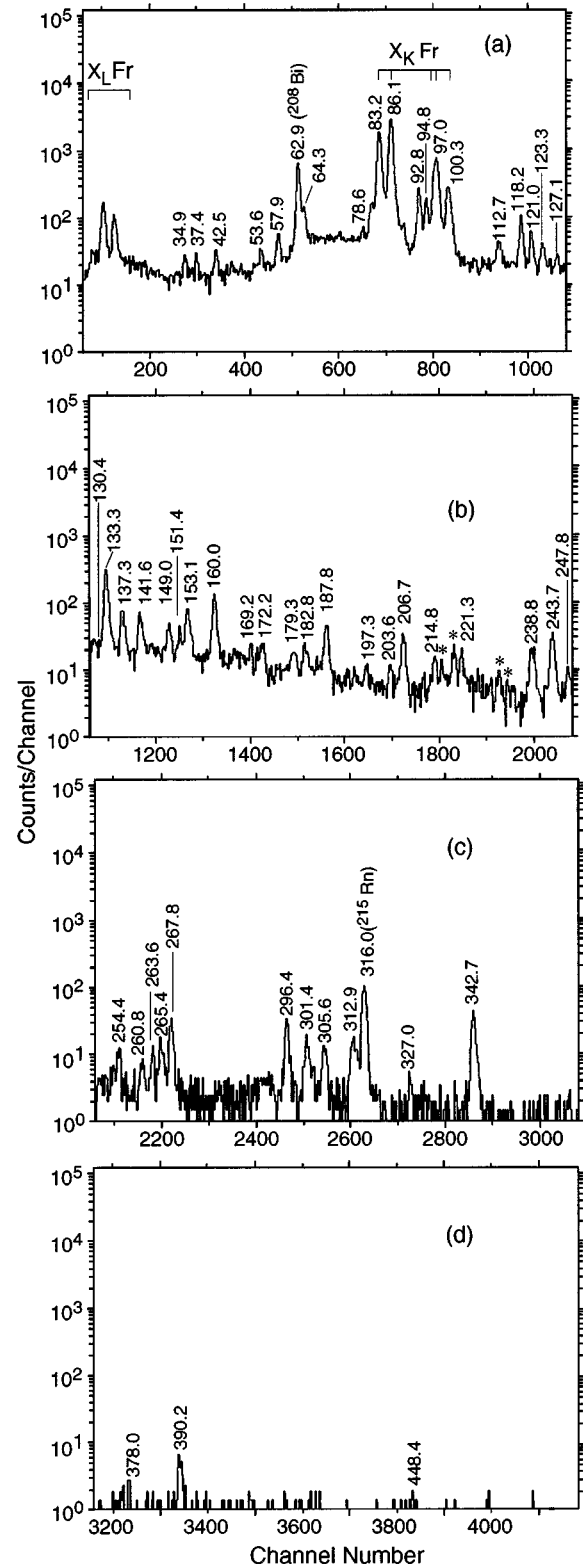


FIG. 2. The gamma spectrum of ^{216}Fr in coincidence with all ^{220}Ac alphas in Fig. 1(b) in four sections. Gamma ray energies are given in keV and x rays indicated.

sents a sequence of gamma spectra [Figs. 4(a)–4(c)] in coincidence with groups of ^{220}Ac alpha lines in which the alpha energies are systematically lowered. This implies that we are moving in the sequence to increasing excitation energies

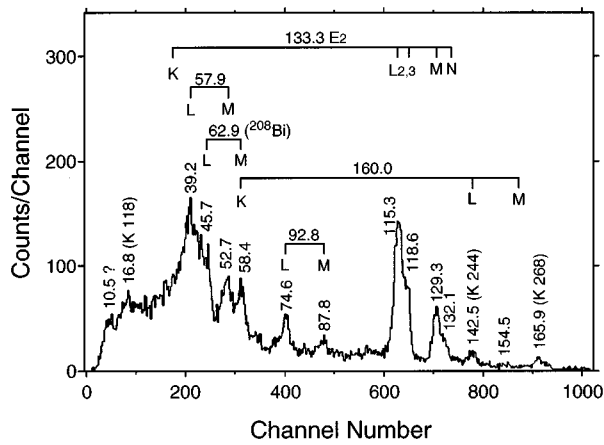


FIG. 3. Conversion electron spectrum of ^{216}Fr in coincidence with the ^{220}Ac alphas of Fig. 1. Electron peaks are labeled by their energies in keV and K, L, M, and N assignments indicated.

in the ^{216}Fr level scheme. The gamma spectrum labeled (a) in Fig. 4 corresponds to gammas in coincidence with 8063 and 8055 keV alphas which populate the 133.3 and 141.6 keV levels; that labeled (b), the 7850 and 7855 keV alphas which populate the 344.2 and 349.2 keV levels; and that labeled (c), the 7792 keV alpha which populates the 409.3 keV level. In a similar way Fig. 5 shows the gamma spectrum in coincidence with alphas from 7622 to 7709 keV which populate the 6 levels, 493.4, 532.0, 539.3, 550.7, 568.7, and 581.4 keV. The energies in keV of the gamma transitions, x-ray transitions, and in some cases (Fig. 5) impurities are indicated in Figs. 4 and 5. In this way we move consistently up the level scheme, watching gammas grow in and then decay out with decreasing alpha energy. One automatically places the levels, the transitions which depopulate them, and, by using the conversion electron spectra of Fig. 3, often determines the multipolarities of the transitions.

Table I lists all gamma rays directly observed, together with their energies, intensities, and multipolarities if determined in these experiments. In addition, Table I indicates the assignment of the observed transitions in the level scheme.

III. THE LEVEL SCHEME OF ^{216}Fr

Using the results of Figs. 1–5 and Table I, the level scheme of ^{216}Fr is proposed in Fig. 6. All levels except the 247.8 keV level, shown dashed in Fig. 6, have been established. 87% of the observed gamma ray intensity and >99.7% of the ^{220}Ac alpha decay has been assigned in the level structure. Vertical arrows show the assigned gamma rays together with their energies and multipolarities when they are available. To the extreme right the energies, intensities, and corresponding hindrance factors (HF's) of the alpha particles are given.

The spin-parity assignments of the two lowest levels (ground state and 133.3 keV) previously assigned [4] are confirmed in the present experiment. The (5^-) assignment of the 191.2 keV state is based on the 57.9 keV $E2$ transition to the 3^- state at 133.3 keV. This transition implies a 5^- or 1^- assignment. However, since it does not decay to the 1^- ground state with much greater transition energy, the (5^-)

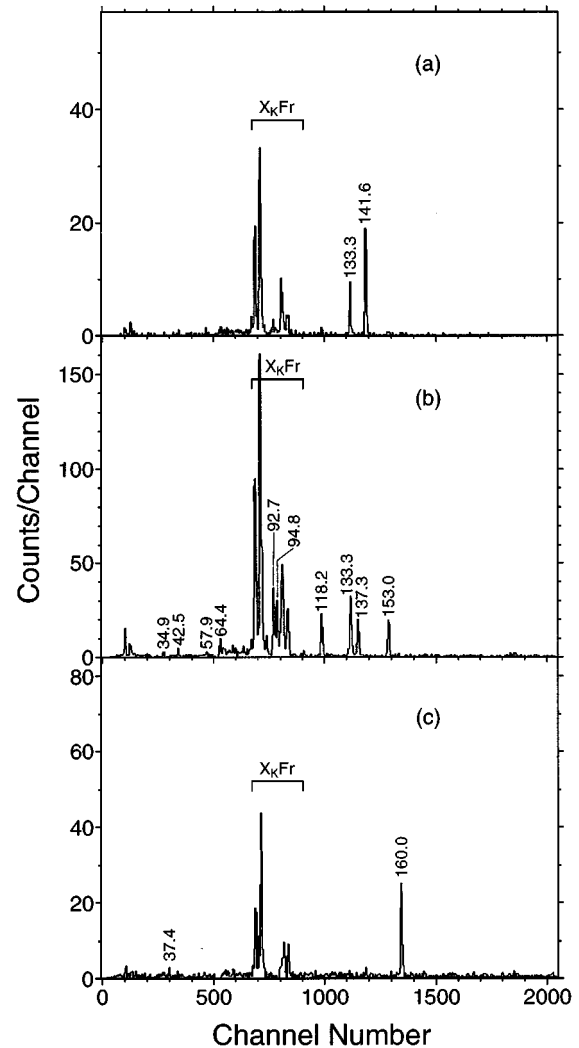


FIG. 4. Gamma ray spectra of ^{216}Fr in coincidence with various ^{220}Ac alpha groups; (a) with 8055–8063 keV alphas; (b) with 7850–7855 keV alphas; (c) with 7792 keV alpha. Gamma ray energies are labeled in keV.

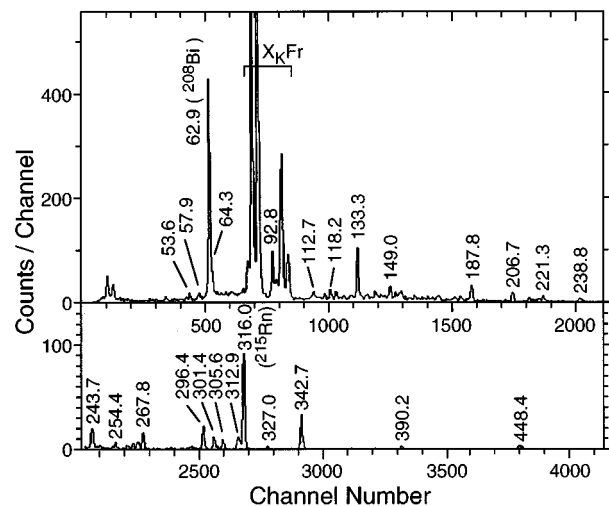


FIG. 5. Gamma ray spectrum of ^{216}Fr in coincidence with 7622 to 7709 keV alphas of ^{220}Ac in two sections with gammas labeled in keV.

TABLE I. Gamma ray transitions in ^{216}Fr following alpha decay of ^{220}Ac .

$E_\gamma(\Delta E_\gamma)$	UCRL 20426(71)	$I_\gamma / 1000_\alpha$	Multi- polarities	Transition	Multipolarities deduction Experimental Values
Present work	E_γ				
34.9 (0.3)		~ 2		226.1 \rightarrow 191.2	
37.4 (0.3)		~ 2		249.3 \rightarrow 211.9	
42.5 (0.2)		~ 3		(254.4 \rightarrow 211.9)	
53.6 (0.2)	54	~ 3		344.2 \rightarrow 290.4	
57.9 (0.1)	60	6.6 ± 2.0	$E2$	191.2 \rightarrow 133.3	$\alpha_L=50\pm 20$
64.3 (0.1)	64	18 ± 3		290.4 \rightarrow 226.1	
78.6 (0.2)	75	5 ± 2		211.4 \rightarrow 133.3	
92.8 (0.1)		37 ± 5	$M1$	226.1 \rightarrow 133.3	$\alpha_L=2.3\pm 0.5$
94.8 (0.1)		25 ± 4		344.2 \rightarrow 249.3	
112.7 (0.3)	113	5.7 ± 2.0			
118.2 (0.2)	119	13.5 ± 3.5	$(M1)$	344.2 \rightarrow 226.1	$\alpha_K>3$
121.0 (0.2)		8.0 ± 1.4		254.4 \rightarrow 133.3	
123.3 (0.3)	124	5.5 ± 1.4		532.0 \rightarrow 409.3	
127.1 (0.4)		~ 3			
130.4 (0.4)		~ 4		539.3 \rightarrow 409.3	
133.3 (0.1)	134	82 ± 7	$E2$	133.3 \rightarrow 0	$(K/L) < 0.2, L_2/L_3=2.0\pm 0.5$
137.3 (0.2)		15.0 ± 3.0		349.2 \rightarrow 211.9	
141.6 (0.2)	142	13.2 ± 3.0	$M1$	141.6 \rightarrow 0	$(X_k/\gamma)=4\pm 1$
149.0 (0.3)	149	9.5 ± 2.8		493.4 \rightarrow 344.2	
151.5 (0.4)		7.0 ± 2.5			
153.1 (0.2)	154	18.2 ± 3.5		344.2 \rightarrow 191.2	
160.0 (0.1)	161	32.7 ± 5.0	$M1$	409.3 \rightarrow 249.3	$(K/L)=5\pm 1$
169.2 (0.3)		4.3 ± 1.1			
172.2 (0.3)	171	5.0 ± 1.3		581.4 \rightarrow 409.3	
179.3 (0.4)		3.8 ± 1.3			
182.8 (0.3)		5.4 ± 1.6		532.0 \rightarrow 349.2	
187.8 (0.2)	188	14.4 ± 3.0		532.0 \rightarrow 344.2	
197.3 (0.5)	199	~ 3			
203.6 (0.5)		~ 3		493.4 \rightarrow 290.4	
206.7 (0.2)	208	12.0 ± 3.0		550.7 \rightarrow 344.2	
214.8 (0.3)	216	5.1 ± 1.6			
221.3 (0.3)		6.2 ± 1.8			
238.8 (0.3)	240	10.5 ± 2.8			
243.7 (0.2)	245	18.0 ± 4.0	$M1$	493.4 \rightarrow 249.3	$\alpha_K=1.1\pm 0.5$
247.8 (0.4)		4.7 ± 1.4			
254.4 (0.5)	256	5.4 ± 1.7		254.4 \rightarrow 0	
260.8 (0.5)		5.0 ± 1.7			
263.6 (0.4)		6.2 ± 2.0			
265.4 (0.4)		9.0 ± 3.0			
267.8 (0.3)	268	18.0 ± 4.0	$M1$	493.4 \rightarrow 226.1	$\alpha_K=1.2\pm 0.5$
296.4 (0.3)	298	20.3 ± 5.0	$M1$	550.7 \rightarrow 254.4	$\alpha_K=0.8\pm 0.4$
301.4 (0.3)	303	13.0 ± 4.2		550.7 \rightarrow 249.3	
305.6 (0.4)	307	10.2 ± 3.8		532.0 \rightarrow 226.1	
312.9 (0.4)	314	14.2 ± 4.0	$(M1)$	539.3 \rightarrow 226.1	$\alpha_K\sim 0.7$
327.0 (0.6)		~ 4		581.4 \rightarrow 254.4	
342.7 (0.3)	344	34.5 ± 5.0	$M1$	568.7 \rightarrow 226.1	$\alpha_K=0.5\pm 0.2$
378.0 (1.0)		~ 2		568.7 \rightarrow 191.2	
390.2 (0.5)	392	6.6 ± 2.5		581.4 \rightarrow 191.2	
448.4 (1.0)		~ 2		581.4 \rightarrow 133.3	

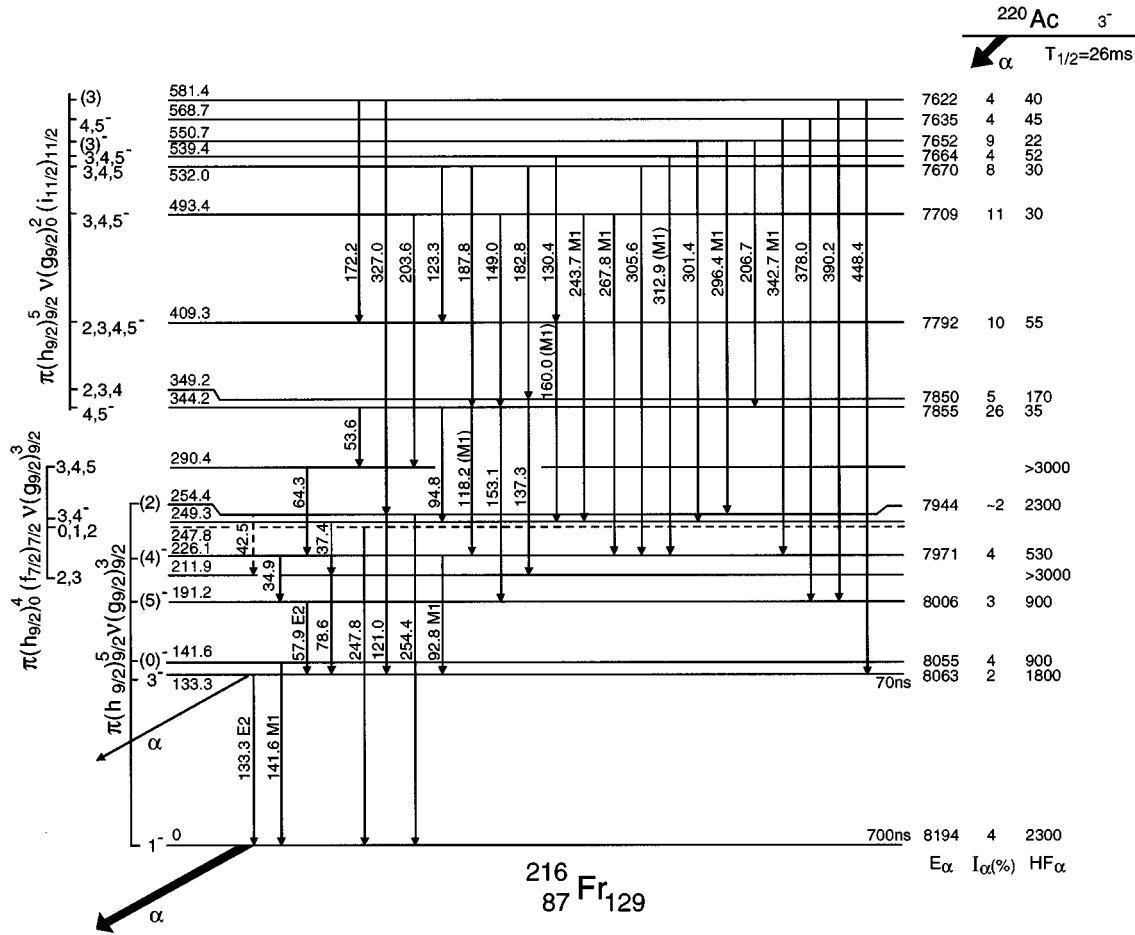


FIG. 6. Energy level scheme of ^{216}Fr resulting from the present study of the ^{220}Ac alpha decay. Alpha energies, intensities, and hindrance factors (HF's) populating levels in ^{216}Fr are shown to the right. Gamma rays are shown as vertical lines together with their energies in keV and multiplicities when known. The resulting level energies, spins, parities, and configurations are given to the left.

spin parity is assigned. The $(4)^-$ assignment of the 226.1 keV state is based on the 92.8 keV $M1$ transition to the 3^- state at 133.3 keV and the 34.9 keV transition to the $(5)^-$ state at 191.2 keV. The $J=(2)$ assignment of the 254.4 keV state is based on the transition to the 3^- 133.3 keV state and the 1^- ground state. The only other state populated in alpha decay with intermediate HF's is the state at 141.6 keV. It is tentatively assigned $(0)^-$ on the basis of the depopulating 141.6 $M1$ transition and the fact that there is no evidence for a transition to the $(0)^-$ state from higher lying states. In a similar way 13 additional states from 211.9 to 581.4 keV are given tentative assignments. In a number of cases the parities of these states can be definitely assigned as negative because of the observed multiplicities of transitions depopulating them. However, the spins are very tentative in all cases. All tentative assignments are internally consistent. However, the state at 581.4 keV requires a quadrupole transition for the 390.2 keV transition populating the $(5)^-$ state at 191.2 keV.

One facet of the spin-parity assignments which proved helpful was the consideration of HF's. It should be noted that for ^{216}Fr they divide into three groupings which are quite separated from each other. The first is from 22 to 170, the second from 530 to 2300, and the third ≥ 3000 . A similar grouping of the HF's proved useful in our understanding of both ^{215}At and ^{217}At [5,6]. In all three cases it appears to be

closely related to the predominant configurations. This point will be further discussed below.

The rationale for the level scheme is presented in Fig. 6. It must be noted, however, that although no other spin-parity sequence is as satisfactory, either experimentally or theoretically as that of Fig. 6, the spins, but not the parities listed in parentheses or with multiple entries are uncertain. However, it should be clearly understood that the level structure including the transitions between states has been established with the possible exception of the tentative level at 247.8 keV. Assuming the correctness of Fig. 6, a number of interesting features of this level scheme are presented in the discussion which follows.

IV. DISCUSSION

A. Shell-model configurations in ^{216}Fr

We expect to see evidence of the $h_{9/2}g_{9/2}$, $f_{7/2}g_{9/2}$, and $h_{9/2}i_{11/2}$ shell-model states in that order in ^{216}Fr . This assumption is based on the level ordering in ^{209}Bi and the theoretical shell model as well as the levels in ^{215}At and ^{217}At [5,6] for the protons, and ^{209}Pb and the shell model for the neutrons. These are the groups of states beginning at the ground state, the 211.9 keV state and the 344.2 keV state in Fig. 6. The complete configurations are $\pi(h_{9/2})^5_{9/2}\nu(g_{9/2})^3_{9/2}$, $\pi(h_{9/2})^4_{9/2}\nu(f_{7/2})_{7/2}\nu(g_{9/2})^3_{9/2}$, and $\pi(h_{9/2})^5_{9/2}\nu(g_{9/2})^2_{9/2}(i_{11/2})_{11/2}$.

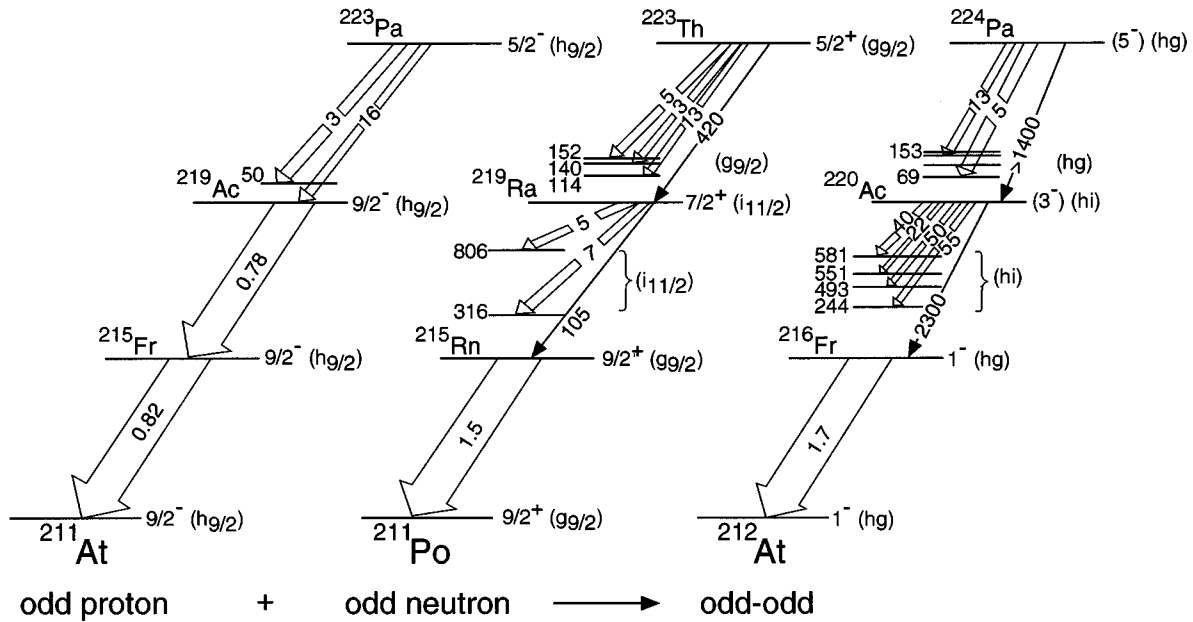


FIG. 7. A diagram comparing the alpha decay chains of $^{223}\text{Pa} \rightarrow ^{211}\text{At}$, $^{223}\text{Th} \rightarrow ^{211}\text{Po}$, and $^{224}\text{Pa} \rightarrow ^{212}\text{At}$. The numbers associated with arrows are hindrance factors (HF's). Only part of the alpha decays are shown. Shell model parentages are also given. The pattern of ^{224}Pa decays mirrors that of the ^{223}Pa decays as expected. See text.

The best evidence for these configurational assignments comes from HF's observed in the alpha decay of the 3^- state in ^{220}Ac [7]. The states of the three configurations are populated in alpha decay with hindrance factors which can be collected into three quite separate groupings. More specifically, the six observed members of the $h_{9/2}g_{9/2}$ configuration have HF's from 800–2300, the four observed members of the $f_{7/2}g_{9/2}$ configuration all have HF's >3000 , while the nine observed members of the $h_{9/2}i_{11/2}$ configuration have HF's from 22–170. While the 3^- ground state of the alpha decaying ^{220}Ac parent has an octupole deformed configuration assignment, its shell model parentage is $h_{9/2}i_{11/2}$. Thus the alpha population of the six members of the ground state configuration is hindered by an $11/2^+ \rightarrow 9/2^+$ transition. In the same way the four members of the $f_{7/2}g_{9/2}$ configuration are much more hindered since both the neutron and the proton are simultaneously required to change configuration. No alpha decay is observed to any of these states and HF limits >3000 are assigned. The nine states comprising the $h_{9/2}i_{11/2}$ configuration are allowed in alpha decay with by far the lowest HF's. Nonetheless it is important to note that these nine states all have spins from two to five. We only expect four such states from the lowest energy part of the $h_{9/2}i_{11/2}$ configuration. Thus we must expect that other states share some of the $h_{9/2}i_{11/2}$ configuration through mixing.

Finally, it is worthwhile mentioning again the coexistence of shell model and collective phenomena which has been pointed out in the extensive study of the isotope ^{218}Ac [8].

B. Comparison of the alpha decays of the ^{223}Pa , ^{223}Th , and ^{224}Pa families

The three alpha decay chains of ^{223}Pa , ^{223}Th , and ^{224}Pa to ^{211}At , ^{211}Po , and ^{212}At , respectively, are shown in Fig. 7. Each of these chains spans the region from the quadrupole-octupole reflection asymmetric region to the shell model re-

flexion symmetric region. The ground state to ground state alpha decay HF's decrease as we go to lower mass numbers in each of the families (although in the case of ^{224}Pa we have only a lower limit on the HF). This systematic occurs because of the collapse of the quadrupole-octupole Nilsson orbitals into the more degenerate shell model orbitals.

An even more interesting aspect of Fig. 7 results when one looks at shell model parentage of each of the families of alpha decays. Thus for example, the shell model parentage of the ground states of the odd proton nuclei ^{223}Pa , ^{219}Ac , ^{215}Fr , and ^{211}At are all $h_{9/2}$. As a result the HF's between these ground states remain small. On the other hand, the shell model parentage of the ground states of the odd neutron nuclei, ^{223}Th , ^{219}Ra , ^{215}Rn , and ^{211}Po switches from $g_{9/2}$ to $i_{11/2}$ and back to $g_{9/2}$ for the last 2 members of the family in Fig. 7. As a result the HF's between the ground states of the first two alpha decays of the ^{223}Th family are quite large whereas small HF's are observed to a group of excited states which have the same shell model parentage as the parent ground states. When the odd proton and odd neutron families are combined into the odd-odd family of ^{224}Pa as indicated at the bottom of Fig. 7, the HF's are what one would expect. The $h_{9/2}$ partial configuration is present in all the configurations and therefore does not influence the systematics of HF's. However, the odd neutron partial configurations switch character from $g_{9/2}$ to $i_{11/2}$ and back to $g_{9/2}$ just as in the case of the ^{223}Th and result in an approximately mirror systematics.

V. CONCLUSIONS

The level structure of ^{216}Fr has been studied following the alpha decay of ^{220}Ac . Eighteen definite levels and one tentative, level are assigned definite, tentative, or multiple spin values. In twelve cases definite negative parity values

can also be assigned. Alpha decay HF's can be grouped into three sets of values of 800–2300, >3000, and 22–170 which correspond to the population of the configurations $\pi(h_{9/2})^5_{9/2}\nu(g_{9/2})^3_{9/2}$, $\pi(h_{9/2})^4_0(f_{7/2})_{7/2}\nu(g_{9/2})^3_{9/2}$, and $\pi(h_{9/2})^5_{9/2}\nu(g_{9/2})^2_0(i_{11/2})_{11/2}$.

The alpha decay (ground state to ground state) HF systematics of the ^{224}Pa family to ^{212}At can be explained assuming the quadrupole-octupole Nilsson orbitals collapse into the more degenerate shell model orbitals.

Comparison of the alpha decay HF systematics of the ^{223}Pa , ^{223}Th , and ^{224}Pa families show an amazing parallel-

ism. This suggests that the odd-odd family of nuclei from ^{224}Pa to ^{212}At may be thought of as a combination of the odd proton family of nuclei from ^{223}Pa to ^{211}At and the odd neutron family of nuclei from ^{223}Th to ^{211}Po .

It should also be noted that there is no evidence in the level structure for reflection asymmetry in the low lying low spin states of ^{216}Fr .

One of (R.K.S.) would like to thank the National Science Foundation for support under contract No. PHY92-07336 with Florida State University and the CSNSM and the IPN at Orsay for their hospitality and joint support.

-
- [1] M. E. Debray, J. Davidson, M. Davidson, A. J. Kreiner, D. Hojman, D. Santos, K. Ahn, D. B. Fossan, Y. Liang, R. Ma, E. S. Paul, W. F. Piel, Jr., and N. Xu, *Phys. Rev. C* **41**, R1895 (1990).
- [2] T. Lönnroth, V. Rahkonen, and B. Fant, *Nucl. Phys.* **A376**, 29 (1982).
- [3] M. J. Martin, *Nucl. Data Sheets* **49**, 83 (1986).
- [4] Agda Artna-Cohen, *Nucl. Data Sheets* **66**, 171 (1992); C. F. Liang, P. Paris, R. K. Sheline, P. Alexa, and A. Gizon (submitted to *Phys. Rev. C*).
- [5] C. F. Liang, P. Paris, and R. K. Sheline, *Phys. Rev. C* **44**, 676 (1991).
- [6] R. K. Sheline, C. F. Liang, and P. Paris, *Phys. Rev. C* **51**, 1192 (1995).
- [7] C. F. Liang, P. Paris, A. Plochocki, E. Ruchowska, A. Gizon, D. Barnéoud, J. Genevey, G. Cata, and R. K. Sheline, *Z. Phys. A* **354**, 153 (1996).
- [8] M. E. Debray, A. J. Kreiner, M. Davidson, J. Davidson, D. Hojman, D. Santos, V. R. Vavin, N. Schulz, M. Aiche, A. Chevallier, J. Chevallier, and J. S. Sens, *Nucl. Phys.* **A568**, 141 (1994).